BBA - General Subjects 1862 (2018) 2862–2868

Contents lists available at ScienceDirect

BBA - General Subjects

journal homepage: www.elsevier.com/locate/bbagen

High-resolution atomic force microscopy visualization of metalloproteins and their complexes

Nikolay A. Barinov[a], Irina I. Vlasova[a], Alexey V. Sokolov[a,c], Valeria A. Kostevich[a,c], Evgeniy V. Dubrovin[a,b,*], Dmitry V. Klinov[a,*]

[a] Federal Research and Clinical Center of Physical-Chemical Medicine, Malaya Pirogovskaya, 1a, Moscow 119435, Russian Federation
[b] Lomonosov Moscow State University, Leninskie gory, 1-2, Moscow 119991, Russian Federation
[c] Institute of Experimental Medicine, Academika Palvova str., 12, Saint Petersburg 197371, Russian Federation

ARTICLE INFO

Keywords:
High-resolution atomic force microscopy
Myeloperoxidase
Ceruloplasmin
Lactoferrin
Metalloprotein complexes
Oxidation stress

ABSTRACT

Background: Metalloproteins myeloperoxidase (MPO), ceruloplasmin (CP) and lactoferrin (LF) play an important role in regulation of inflammation and oxidative stress in vertebrates. It was previously shown that these proteins may work synergetically as antimicrobial and anti-inflammatory agents by forming complexes, such as MPO-CP and LF-CP. However, interaction of metalloprotein molecules with each other has never been characterized at a single-molecule level.

Methods: In this study, the pairwise interactions of MPO, CP and LF molecules were investigated at a single-molecule level using high-resolution atomic force microscopy (AFM). Highly oriented pyrolytic graphite surface (HOPG) modified with oligoglycine-hydrocarbon graphite modifier (GM) was used as a substrate for protein deposition.

Results: The procedure for reliable AFM investigation of metalloproteins and their complexes has been developed. Using this procedure, we have visualized, for the first time, single MPO, CP and LF molecules, characterized the morphology of MPO-CP and LF-CP complexes and confirmed the absence of direct contacts between MPO and LF molecules. Moreover, we have revealed the novel chainlike shape of MPO-CP conjugates.

Conclusions: GM-HOPG was shown to be a convenient substrate for AFM investigation of metalloproteins and their complexes. Direct AFM visualization of MPO-CP and LF-CP complexes, on the one hand, complements previous data obtained from the "bulk techniques" and, on the other hand, provides new insight into the ultrastructure of MPO-CP complexes.

General significance: The obtained results contribute to the better understanding of regulation of inflammation and oxidation stress mediated by collaborative action of the metalloproteins such as MPO, CP and LF.

1. Introduction

Myeloperoxidase (MPO), ceruloplasmin (CP) and lactoferrin (LF) are metalloproteins, which play an important role in regulation of inflammation and oxidative stress in vertebrates. The proteins were demonstrated to form binary and ternary complexes and affect the enzymatic activities of each other [1–3].

MPO is a globular cationic (pI ~10.7) heme-containing homodimeric enzyme with molecular mass of ~140 kDa. It is a major protein of neutrophilic leukocytes. MPO is secreted by activated neutrophils into phagosomes and extracellular space and protects the body from invading pathogens due to its unique ability to generate hypochlorous acid (HOCl) – a highly cytotoxic oxidizing agent [4,5]. The interaction of highly cationic MPO with anionic proteins and with the negatively charged surfaces of different cells has been suggested to be mostly dependent on electrostatic interactions [6].

CP is a globular anionic (pI ~4.4) copper containing plasma glycoprotein with molecular mass of ~132 kDa. It has multiple functions, the major of which is participation in iron metabolism by oxidizing Fe^{2+} to Fe^{3+} [7]. Moreover, CP plays an important role as a physiological inhibitor of peroxidase activity of MPO [1,8,9]. The mechanism of this inhibition implies strong electrostatic binding (with dissociation constant of ~0.15 μM) of CP with MPO at the ratio 1:1 or 2:1 [1,2]. CP binds in the close proximity of MPO active site and forms a steric barrier impeding binding of substrates to MPO [1,10]. Significant increase of CP content in blood plasma upon inflammation [11] is

* Corresponding authors at: Federal Research and Clinical Center of Physical-Chemical Medicine, Malaya Pirogovskaya, 1a, Moscow 119435, Russian Federation.
E-mail addresses: dubrovin@polly.phys.msu.ru (E.V. Dubrovin), klinov.dmitry@mail.ru (D.V. Klinov).

https://doi.org/10.1016/j.bbagen.2018.09.008
Received 3 May 2018; Received in revised form 17 August 2018; Accepted 11 September 2018
Available online 12 September 2018

believed to protect an organism from unfavorable excessive MPO activity.

LF is a globular cationic glycoprotein (pI ~8.5) which belongs to a transferrin family. The protein was first described as a breast milk major protein, it could be also found in exocrine secretions and in specific granules of neutrophils. It consists of two homological chains and has a molecular mass of ~78 kDa. Among many functions of LF is the control of iron metabolism in an organism, immunomodulating, antiinflammatory and antimicrobial activities. LF does not establish direct contacts with MPO (they are both cationic proteins), however, these proteins may work synergetically as antimicrobial agents by forming triple complexes with CP (2CP-2LF-MPO) [2,12].

Though interaction of MPO, CP and LF has been characterized by a variety of physicochemical methods, including small angle X-ray scattering, surface plasmon resonance, chromatography, gel-electrophoresis etc. [2,12–15], the data obtained from single molecules or complexes at a subnanometer level are still absent. Such data may complement the existing knowledges concerning the properties of the metalloproteins, their interaction with each other and with different biologically relevant surfaces.

Atomic force microscopy (AFM) is one of the most appropriate techniques for investigation of the morphology and properties of single protein molecules and their complexes at a subnanometer scale [16–22]. Since AFM requires the immobilization of a studied protein onto a solid substrate, utilization of substrate surfaces retaining the native structure of the adsorbed proteins is of great importance. Recently, we have demonstrated that the surface of highly oriented pyrolytic graphite (HOPG) modified with oligoglycine hydrocarbon graphite modifier (GM) retains nativelike structure and dimensions of the adsorbed proteins, such as ferritin, fibrinogen, immunoglobulin G and RNA polymerase [19,23]. It was suggested that GM-HOPG surface may be used as a convenient substrate for AFM investigation of other protein molecules and their complexes. The AFM measured height of globular proteins (such as metalloproteins) can be used as a characteristic value to distinguish different protein molecules and their complexes.

Therefore, in this work, first of all, we aimed to characterize the conformation and stability of single MPO, CP and LF molecules adsorbed on a GM-HOPG surface using high-resolution AFM and to elaborate the procedure for AFM investigation of the metalloproteins and their complexes. Moreover, we intended to study the pairwise interactions of MPO, CP and LF at a single molecule level and to visualize MPO-CP and CP-LF complexes using AFM.

2. Experimental section

MPO was purchased from Planta Natural Products (Vienna, Austria).

Homogeneous non-proteolyzed ceruloplasmin was obtained by original scheme worked out previously by using ion-exchange chromatography of human blood plasma on UNO Sphere Q to isolate CP and by affinity chromatography on neomycin-agarose for extra purification of CP [24]. Partially proteolyzed CP (ppCP) was obtained by thrombin limited proteolysis [25].

LF was purified from breast milk using ion-exchange chromatography on CM-Sepharose and gel filtration on Sephadex G-75 Superfine [3].

2.1. Sample preparation for AFM

For preparation of a GM-HOPG surface, 10 µl of GM ($(CH_2)_n(NCH_2CO)_m$-NH_2 [26,27], Nanotuning, Russia) solution in deionized and distilled water at a concentration 0.01 mg/ml was placed onto freshly cleaved HOPG (ZYB quality, NT-MDT, Russia) surface for 1 min. After that the droplet of GM solution was removed from the surface by a nitrogen flow.

MPO, CP and LF was diluted by 10 mM sodium phosphate buffer (pH 7.2) to a final concentration 0.5 µM. For protein deposition, 1 µl of MPO, CP or LF solution was placed onto a GM-HOPG surface for 10 s. After that, 100 µl of water was added on top of the sample and removed immediately by a nitrogen flow.

For AFM investigation of the pairwise interactions of MPO, CP and LF, the protein solutions (1 µM) of each two of them were mixed at a molar ratio 1:1 (and for the case MPO-CP also at a molar ratio 2:1) and incubated for 3 min. The deposition of the MPO-CP, MPO-LF or CP-LF mixtures onto a GM-HOPG surface was the same as for the proteins.

2.2. AFM

In order to avoid possible surface induced protein unfolding [28] and obtain better spatial resolution of AFM images of proteins [29], all AFM measurements were conducted in air. We have used the multimode atomic force microscope Ntegra Prima (NT-MDT, Russia) equipped by the ultra-sharp cantilevers (carbon nanowhiskers with a curvature radius of several nanometers grown at tips of commercially available silicon cantilevers with a spring constant of 5–30 N/m) [30] and operated in attraction regime of intermittent contact mode at a scan rate of 1 Hz. The typical pixel resolution was ≈1 pixel/nm. For standard AFM image processing and presentation we have used FemtoScan Online (Advanced technologies center, Russia). SPM Image Magic (http://spm-image-magic.software.informer.com) was used for height analysis. It has contained the following steps: identification of objects (metalloprotein molecules or complexes) as local maximums in an AFM image, calculation of height of a protein molecule in respect to the local background surrounding it, and manual filtering of the results of automatic analysis obtained in the previous two steps. All experiments were reproduced at least three times.

3. Results and discussions

3.1. Characterization of single MPO, CP and LF molecules

AFM images of MPO molecules adsorbed onto a GM HOPG surface (Fig. 1a) represent globules with an extended shape (the inset depicts the enlarged MPO molecule) that conforms with the available crystal structure of human MPO: it has an extended and flattened shape with longitudinal dimension of ≈11 nm and transverse dimensions varying from 4 to 7 nm [31]. The height distribution of MPO (Fig. 1b) demonstrates the mean value of 4.0 ± 0.3 nm (N = 290). This size approximately corresponds to the smallest dimension of a molecule across its “length”, therefore, indicating a “flat-on” orientation of MP molecules adsorbed on a GM-HOPG surface. No signs of protein denaturation are observed.

AFM images of CP molecules adsorbed onto a GM HOPG surface (Fig. 1c) demonstrate globules with mean height of 5.0 ± 0.3 nm (N = 184). The left inset depicts the enlarged CP molecule. The obtained height is in agreement with the crystallographic structure of CP, whose overall sizes vary from ~5 to 8 nm in different directions [2,32,33]. The presence of a protein fraction with smaller heights (down to ~3 nm; see the height distribution in Fig. 1d) may be connected with the existence of “spontaneously” degraded CP [34]. The possible example of a degraded molecule is enlarged in the right inset in Fig. 1c. Recently, CP degradation was explained by its proteolysis induced by thrombin, always present in blood plasma [35].

AFM images of LF adsorbed onto GM HOPG surface represent globules with the mean height of 2.9 ± 0.5 nm (N = 324) (Fig. 1e), which in view of its crystallographic structure [36] indicates a “flat-on” orientation of LF molecules on the surface. The characteristic height distributions of LF, CP and MPO (Fig. 1b,d,f) almost do not intersect with each other providing an opportunity to discern three proteins in the mixtures by their height obtained from AFM images.

The examples of AFM height profiles along single metalloprotein molecules are shown in the Supplementary material (fig. S1). The mean

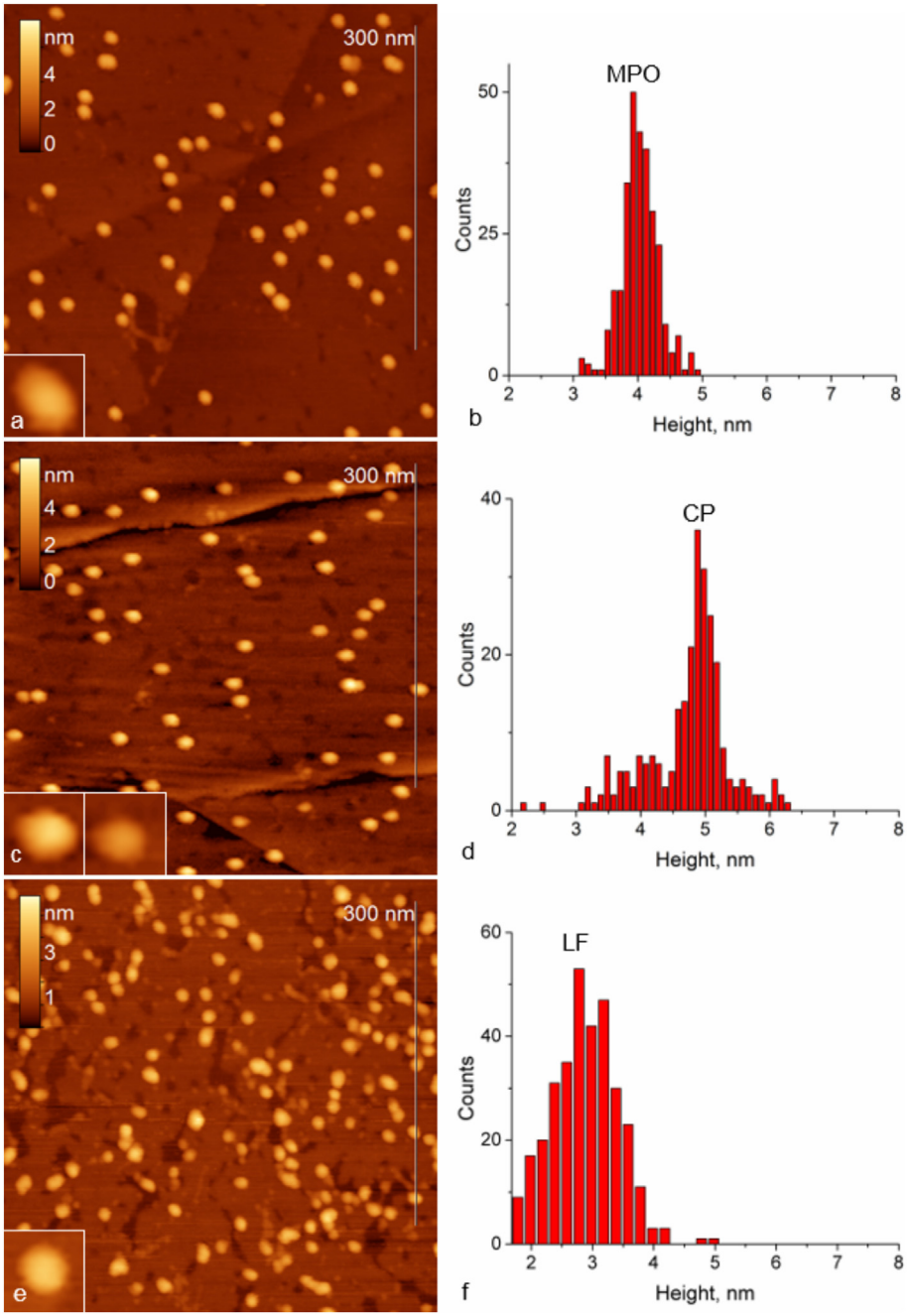

Fig. 1. (a, c, e) AFM images and (b, d, f) height distribution histograms of (a, b) MPO, (c, d) CP and (e, f) LF adsorbed onto a GM-HOPG surface. Insets demonstrate enlarged images of protein molecules. The size of AFM images is 400 × 400 nm^2 (insets 20 × 20 nm^2).

Table 1
AFM measured mean height values of MPO, CP, LF and their binary complexes adsorbed onto a GM-HOPG surface (the number of molecules is shown in brackets).

Protein or protein complex	Height, nm
MPO	4.0 ± 0.3 (290)
CP	5.0 ± 0.3 (184)
LF	2.9 ± 0.5 (324)
MPO-CP	6.5 ± 0.3 (417)
MPO-LF	not formed
LF-CP	6.5 ± 0.4 (272)

AFM measured heights of MPO, CP and LF molecules are summarized in Table 1. They are smaller by a factor of 1.5–2 than their hydrodynamic diameters defined by dynamic light scattering [2]. This may be connected with different factors such as flat-on orientation of the adsorbed asymmetric protein molecules on the substrate, the influence of local probe-sample geometry [37], and protein deformation induced by an AFM probe.

3.2. Characterization of MPO-CP complexes

For AFM visualization of MPO-CP complexes we have prepared them by incubation of MPO and CP at the molar ratio 1:1 and 2:1 and deposited onto a GM-HOPG surface (see Experimental section for details). AFM images of 1:1 MPO-CP mixture (Fig. 2a) contain globules of

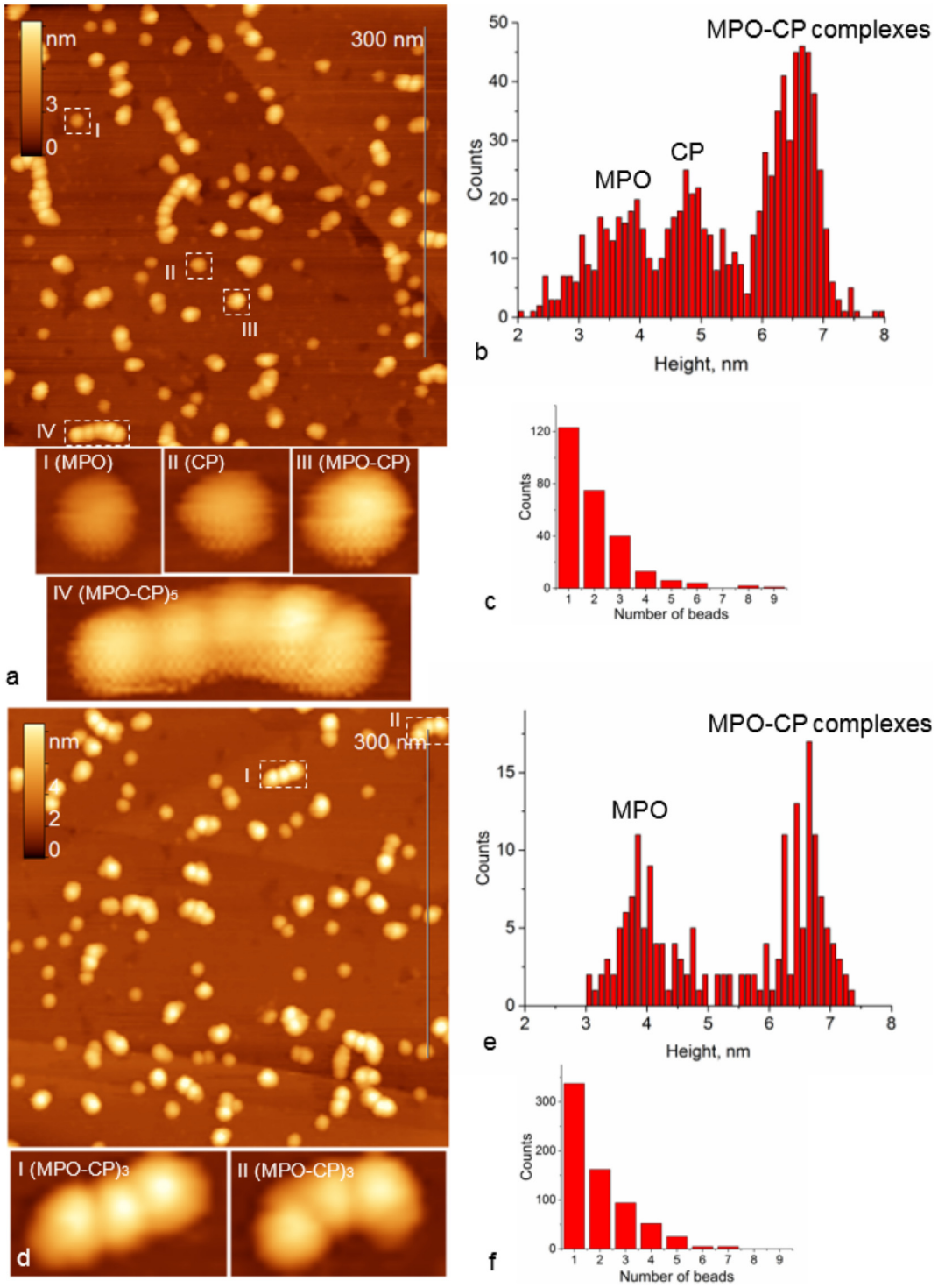

Fig. 2. (a, d) AFM images and (b, e) height distribution histograms of MPO-CP mixture obtained at the molar ratio (a, b) 1:1 and (d, e) 2:1. Insets demonstrate enlarged images of MPO, CP protein molecules or their complexes (the corresponding regions are marked with Roman numbers near dashed squares/rectangles). The size of AFM images is 400 × 400 nm^2 (insets 20 × 20 nm^2, 20 × 60 nm^2 (a) and 25 × 45 nm^2 (d)). (c, f) The distributions of the number of beads in MPO-CP complexes.

different heights (examples are enlarged in the insets I-III). Moreover, chains of globules can be revealed in AFM images (inset IV). Height distribution histogram (Fig. 2b) contains peaks around 4 and 5 nm, which according to Fig. 1 may correspond to MPO and CP. Furthermore, the new maximum centered at ~6.5 nm is observed. It can be assigned to MPO-CP complexes. These complexes are present either as single globules (e.g., inset III) or chains of several globules (e.g., inset IV), which we call supercomplexes. Their chainlike structure confirms that the complexes may aggregate through the specific binding sites of MPO and CP that were identified earlier [12]. The number of globules (complexes) within one supercomplex varied from 2 to 9 in our experiments (Fig. 2c). The examples of AFM height profiles along MPO, CP molecules and MPO-CP complexes are shown in the Supplementary material (fig. S2).

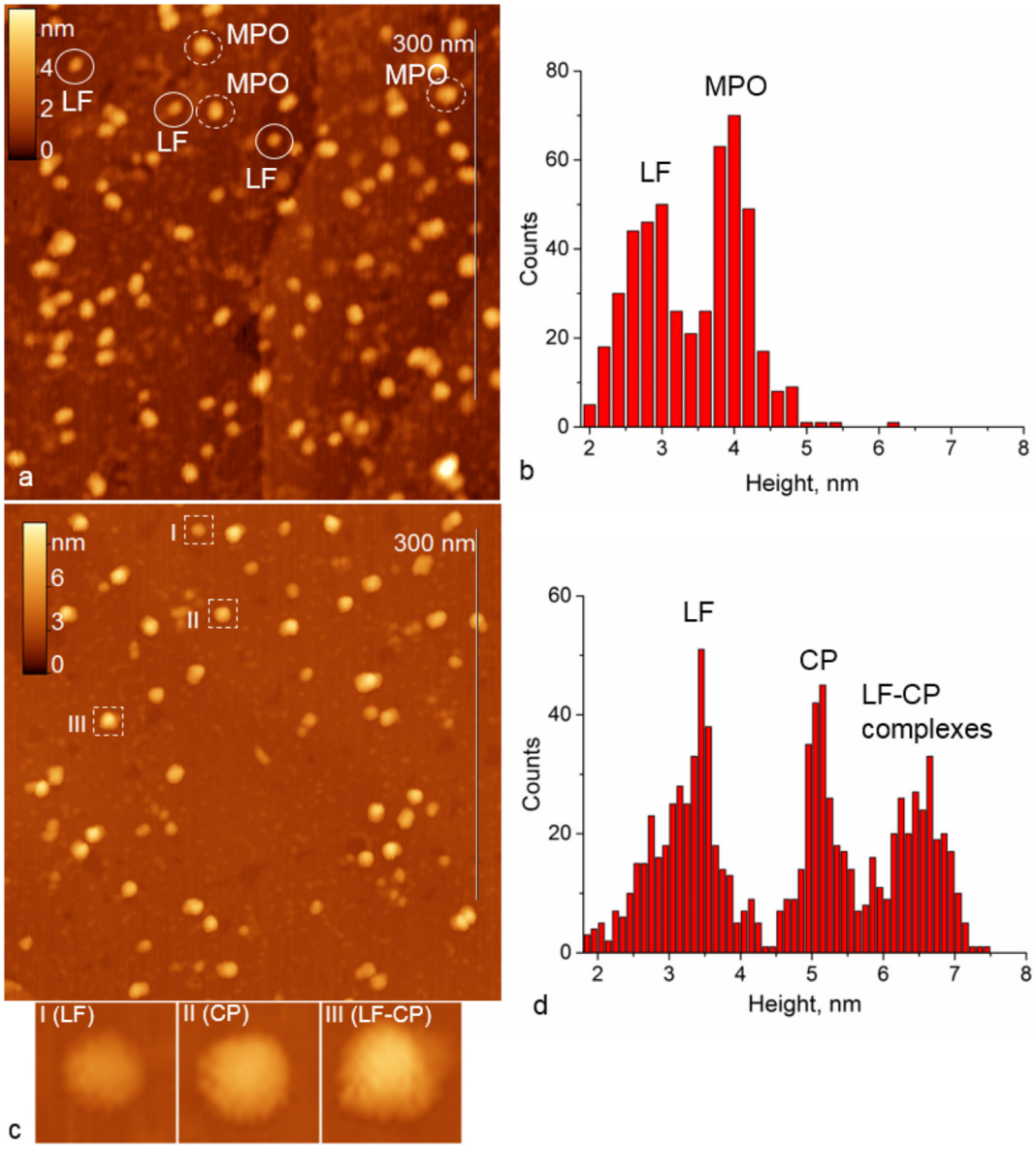

Fig. 3. (a,c) AFM images and (b,d) height distribution histograms of (a, b) MPO-LF and (c, d) CP-LF mixture obtained at the molar ratio 1:1. Insets demonstrate enlarged images of LF, CP molecules or their complexes (the corresponding regions are marked with Roman numbers near dashed rectangles). The size of AFM images is 400 × 400 nm^2 (insets 20 × 20 nm^2).

AFM images obtained for 2:1 MPO-CP mixture deposited onto a GM-HOPG surface have also revealed the presence of globules of different heights as well as chains of globules (Fig. 2d) similar to those obtained for a 1:1 MPO-CP mixture. However, the histogram of height distribution of the observed objects (Fig. 2e) has only two pronounced maximums: around 4 nm and 6.5 nm. At the same time the middle peak (around 5 nm) is almost absent. This result may be explained as follows: due to the excess of MPO in the mixture (maximum at ~4 nm), all CP goes into MPO-CP complexes (maximum at ~6.5 nm) and, therefore, CP alone (with characteristic height of about 5 nm) cannot be observed in the AFM images. This interpretation gives the additional evidence that the first two maximums in the height distribution of 1:1 MPO-CP mixture (Fig. 2b) correspond to MPO and CP molecules, whereas the third one – to their complexes. The MPO-CP complexes in 2:1 MPO-CP mixture exist both in the form of single globules and supercomplexes (two supercomplexes are enlarged in the insets I and II in Fig. 2d). The distribution of the number of beads within one supercomplex (Fig. 2f) is similar to that obtained for 1:1 MPO-CP mixture.

It is known that partially proteolyzed CP (ppCP) loses the ability to inhibit MPO [1]. Though AFM images have revealed the presence MPO-ppCP complexes at a molar ratio 2:1, their quantity was significantly lower than for native CP (Supplementary material, fig. S3a,b). Moreover, most complexes were formed as single globules, and only small fraction of them was observed in the form of supercomplexes, usually quite short (Supporting information, fig. S3c). This demonstrates that ppCP has reduced capability to form supercomplexes with MPO.

3.3. Characterization of LF-MPO and LF-CP mixtures

Typical AFM image of LF-MPO mixture is shown in Fig. 3a. It contains different globules, which depending on their heights may be attributed either to LF or to MPO. Three examples of each type of protein molecules are encircled in Fig. 3a by a solid (LF) and dashed (MPO) lines. Height distribution histogram of the LF-MPO mixture (Fig. 3b) resembles two maximums around 3 and 4 nm, which comply with the distributions of the corresponding components of the mixture (i.e. MPO and LF, Fig. 1b,f). Complex formation between MPO and LF cannot be detected neither from the AFM images of their mixture nor from the

corresponding height distribution. This result agrees well with the previous findings obtained by different methods [2,12].

AFM images of LF mixed with CP at a molar ratio 1:1 (Fig. 3c) reveals the presence of globules, whose height distribution (Fig. 3d) allows to distinguish single LF (mean height 3.2 ± 0.4 nm, $N = 355$) and CP (mean height 5.1 ± 0.2 nm, $N = 236$) molecules as well as their complexes (mean height 6.5 ± 0.4 nm, $N = 272$). The examples of single LF, CP molecules and LF-CP complexes are marked in the AFM image and enlarged at the bottom of Fig. 3c.

The examples of AFM height profiles along LF, MPO, CP molecules and LF-CP complexes are shown in the Supplementary material, fig. S4. The mean AFM measured heights of MPO-CP and LF-CP complexes are summarized in Table 1.

4. Conclusions

Using high-resolution AFM, we have visualized, for the first time, single MPO, CP and LF molecules, characterized the morphology of MPO-CP and LF-CP complexes and confirmed the absence of direct contacts between MPO and LF molecules. We have shown that a GM-HOPG surface does not significantly influence the conformation of adsorbed metalloproteins and, in particular, does not induce denaturation effects. Moreover, we have revealed the formation of MPO-CP supercomplexes, composed of several MPO-CP complexes arranged in a chainlike structure. The obtained results contribute to the better understanding of regulation of inflammation and oxidative stress mediated by collaborative action of the metalloproteins such as MPO, CP and LF.

Acknowledgments

This work was supported by the Russian Science Foundation [17-75-30064 to D.V.K.]

Appendix A. Supplementary data

Supplementary data to this article can be found online at https://doi.org/10.1016/j.bbagen.2018.09.008.

References

[1] A.V. Sokolov, K.V. Ageeva, M.O. Pulina, O.S. Cherkalina, V.R. Samygina, I.I. Vlasova, O.M. Panasenko, E.T. Zakharova, V.B. Vasilyev, Ceruloplasmin and myeloperoxidase in complex affect the enzymatic properties of each other, Free Radic. Res. 42 (2008) 989–998, https://doi.org/10.1080/10715760802566574.
[2] A.V. Sokolov, V.N. Prozorovskii, V.B. Vasilyev, Study of interaction of ceruloplasmin, lactoferrin, and myeloperoxidase by photon correlation spectroscopy, Biochem. Mosc. 74 (2009) 1225, https://doi.org/10.1134/S0006297909110078.
[3] A.V. Sokolov, E.T. Zakahrova, V.A. Kostevich, V.R. Samygina, V.B. Vasilyev, Lactoferrin, myeloperoxidase, and ceruloplasmin: complementary gearwheels cranking physiological and pathological processes, Biometals 27 (2014) 815–828, https://doi.org/10.1007/s10534-014-9755-2.
[4] S.J. Klebanoff, Myeloperoxidase: friend and foe, J. Leukoc. Biol. 77 (2005) 598–625, https://doi.org/10.1189/jlb.1204697.
[5] I.I. Vlasova, A.V. Sokolov, J. Arnhold, The free amino acid tyrosine enhances the chlorinating activity of human myeloperoxidase, J. Inorg. Biochem. 106 (2012) 76–83, https://doi.org/10.1016/j.jinorgbio.2011.09.018.
[6] L. Kubala, H. Kolářová, J. Víteček, S. Kremserová, A. Klinke, D. Lau, A.L.P. Chapman, S. Baldus, J.P. Eiserich, The potentiation of myeloperoxidase activity by the glycosaminoglycan-dependent binding of myeloperoxidase to proteins of the extracellular matrix, Biochim. Biophys. Acta Gen. Subj. 1830 (2013) 4524–4536, https://doi.org/10.1016/j.bbagen.2013.05.024.
[7] P. Bielli, L. Calabrese, Structure to function relationships in ceruloplasmin: a "moonlighting" protein, Cell. Mol. Life Sci. CMLS 59 (2002) 1413–1427, https://doi.org/10.1007/s00018-002-8519-2.
[8] M. Segelmark, B. Persson, T. Hellmark, J. Wieslander, Binding and inhibition of myeloperoxidase (MPO): a major function of ceruloplasmin? Clin. Exp. Immunol. 108 (1997) 167–174, https://doi.org/10.1046/j.1365-2249.1997.d01-992.x.
[9] Y.S. Park, K. Suzuki, S. Mumby, N. Taniguchi, J.M.C. Gutteridge, Antioxidant binding of caeruloplasmin to myeloperoxidase: myeloperoxidase is inhibited, but oxidase, peroxidase and immunoreactive properties of caeruloplasmin remain intact, Free Radic. Res. 33 (2000) 261–265, https://doi.org/10.1080/10715760000301421.
[10] V.R. Samygina, A.V. Sokolov, G. Bourenkov, M.V. Petoukhov, M.O. Pulina, E.T. Zakharova, V.B. Vasilyev, H. Bartunik, D.I. Svergun, Ceruloplasmin: macromolecular assemblies with iron-containing acute phase proteins, PLoS One 8 (2013) e67145, , https://doi.org/10.1371/journal.pone.0067145.
[11] J.D. Gitlin, Transcriptional regulation of ceruloplasmin gene expression during inflammation, J. Biol. Chem. 263 (1988) 6281–6287.
[12] A.V. Sokolov, M.O. Pulina, K.V. Ageeva, M.I. Ayrapetov, M.N. Berlov, G.N. Volgin, A.G. Markov, P.K. Yablonsky, N.I. Kolodkin, E.T. Zakharova, V.B. Vasilyev, Interaction of ceruloplasmin, lactoferrin, and myeloperoxidase, Biochem. Mosc. 72 (2007) 409–415, https://doi.org/10.1134/S0006297907040074.
[13] A. Sabatucci, P. Vachette, V.B. Vasilyev, M. Beltramini, A. Sokolov, M. Pulina, B. Salvato, C.B. Angelucci, M. Maccarrone, I. Cozzani, E. Dainese, Structural characterization of the ceruloplasmin: lactoferrin complex in solution, J. Mol. Biol. 371 (2007) 1038–1046, https://doi.org/10.1016/j.jmb.2007.05.089.
[14] K.N. White, C. Conesa, L. Sánchez, M. Amini, S. Farnaud, C. Lorvoralak, R.W. Evans, The transfer of iron between ceruloplasmin and transferrins, Biochim. Biophys. Acta Gen. Subj. 1820 (2012) 411–416, https://doi.org/10.1016/j.bbagen.2011.10.006.
[15] A.V. Sokolov, I.V. Voynova, V.A. Kostevich, A.Y. Vlasenko, E.T. Zakharova, V.B. Vasilyev, Comparison of interaction between ceruloplasmin and lactoferrin/transferrin: to bind or not to bind, Biochem. Mosc. 82 (2017) 1073–1078, https://doi.org/10.1134/S0006297917090115.
[16] M.E. Fuentes-Perez, M.S. Dillingham, F. Moreno-Herrero, AFM volumetric methods for the characterization of proteins and nucleic acids, Methods 60 (2013) 113–121, https://doi.org/10.1016/j.ymeth.2013.02.005.
[17] M.B. Viani, L.I. Pietrasanta, J.B. Thompson, A. Chand, I.C. Gebeshuber, J.H. Kindt, M. Richter, H.G. Hansma, P.K. Hansma, Probing protein–protein interactions in real time, Nat. Struct. Mol. Biol. 7 (2000) 644–647, https://doi.org/10.1038/77936.
[18] O.N. Koroleva, E.V. Dubrovin, I.V. Yaminsky, V.L. Drutsa, Effect of DNA bending on transcriptional interference in the systems of closely spaced convergent promoters, Biochim. Biophys. Acta Gen. Subj. 1860 (2016) 2086–2096, https://doi.org/10.1016/j.bbagen.2016.06.026.
[19] E.V. Dubrovin, M. Schächtele, D.V. Klinov, T.E. Schäffer, Time-lapse single-biomolecule atomic force microscopy investigation on modified graphite in solution, Langmuir 33 (2017) 10027–10034, https://doi.org/10.1021/acs.langmuir.7b02220.
[20] M. Pfreundschuh, D. Martinez-Martin, E. Mulvihill, S. Wegmann, D.J. Muller, Multiparametric high-resolution imaging of native proteins by force-distance curve–based AFM, Nat. Protoc. 9 (2014) 1113–1130, https://doi.org/10.1038/nprot.2014.070.
[21] Y.F. Dufrêne, D. Martínez-Martín, I. Medalsy, D. Alsteens, D.J. Müller, Multiparametric imaging of biological systems by force-distance curve–based AFM, Nat. Methods 10 (2013) 847–854, https://doi.org/10.1038/nmeth.2602.
[22] S. Ido, H. Kimiya, K. Kobayashi, H. Kominami, K. Matsushige, H. Yamada, Immunoactive two-dimensional self-assembly of monoclonal antibodies in aqueous solution revealed by atomic force microscopy, Nat. Mater. 13 (2014) 264–270, https://doi.org/10.1038/nmat3847.
[23] N.A. Barinov, V.V. Prokhorov, E.V. Dubrovin, D.V. Klinov, AFM visualization at a single-molecule level of denaturated states of proteins on graphite, Colloids Surf. B: Biointerfaces 146 (2016) 777–784, https://doi.org/10.1016/j.colsurfb.2016.07.014.
[24] A.V. Sokolov, V.A. Kostevich, D.N. Romanico, E.T. Zakharova, V.B. Vasilyev, Two-stage method for purification of ceruloplasmin based on its interaction with neomycin, Biochem. Mosc. 77 (2012) 631–638, https://doi.org/10.1134/S0006297912060107.
[25] E.A. Golenkina, G.M. Viryasova, S.I. Galkina, T.V. Gaponova, G.F. Sud'ina, A.V. Sokolov, Fine regulation of neutrophil oxidative status and apoptosis by ceruloplasmin and its derivatives, Cell 7 (2018) 8, https://doi.org/10.3390/cells7010008.
[26] N.V. Bovin, D.V. Klinov, Method for Modifying Hydrophobic Surfaces, WO2007011262A3, https://patents.google.com/patent/WO2007011262A3/en, (2007).
[27] D.V. Klinov, N.V. Bovin, Method of Modification of the Hydrophobic Surfaces, 2305592, http://www.freepatent.ru/images/patents/158/2305592/patent-2305592.pdf, (2007).
[28] N.A. Barinov, A.D. Protopopova, E.V. Dubrovin, D.V. Klinov, Thermal denaturation of fibrinogen visualized by single-molecule atomic force microscopy, Colloids Surf. B: Biointerfaces 167 (2018) 370–376, https://doi.org/10.1016/j.colsurfb.2018.04.037.
[29] S. Santos, N.H. Thomson, High resolution imaging of immunoglobulin G antibodies and other biomolecules using amplitude modulation atomic force microscopy in air, Atomic Force Microscopy in Biomedical Research, Humana Press, 2011, pp. 61–79, , https://doi.org/10.1007/978-1-61779-105-5_5.
[30] D. Klinov, S. Magonov, True molecular resolution in tapping-mode atomic force microscopy with high-resolution probes, Appl. Phys. Lett. 84 (2004) 2697–2699, https://doi.org/10.1063/1.1697629.
[31] R. Fenna, J. Zeng, C. Davey, Structure of the green heme in myeloperoxidase, Arch. Biochem. Biophys. 316 (1995) 653–656, https://doi.org/10.1006/abbi.1995.1086.
[32] I. Bento, C. Peixoto, V.N. Zaitsev, P.F. Lindley, Ceruloplasmin revisited: structural and functional roles of various metal cation-binding sites, Acta Crystallogr. D Biol. Crystallogr. 63 (2007) 240–248, https://doi.org/10.1107/S090744490604947X.
[33] V.R. Samygina, A.V. Sokolov, M.O. Pulina, H.D. Bartunik, V.B. Vasil'ev, X-ray diffraction study of highly purified human ceruloplasmin, Crystallogr. Rep. 53 (2008) 655, https://doi.org/10.1134/S1063774508040172.
[34] I.B. Kingston, B.L. Kingston, F.W. Putnam, Chemical evidence that proteolytic cleavage causes the heterogeneity present in human ceruloplasmin preparations, Proc. Natl. Acad. Sci. U. S. A. 74 (1977) 5377–5381.

[35] A.V. Sokolov, L. Acquasaiente, V.A. Kostevich, R. Frasson, E.T. Zakharova, G. Pontarollo, V.B. Vasilyev, V. De Filippis, Thrombin inhibits the anti-myeloperoxidase and ferroxidase functions of ceruloplasmin: relevance in rheumatoid arthritis, Free Radic. Biol. Med. 86 (2015) 279–294, https://doi.org/10.1016/j.freeradbiomed.2015.05.016.

[36] H.M. Baker, C.J. Baker, C.A. Smith, E.N. Baker, Metal substitution in transferrins: specific binding of cerium(IV) revealed by the crystal structure of cerium-substituted human lactoferrin, JBIC J. Biol. Inorg. Chem. 5 (2000) 692–698, https://doi.org/10.1007/s007750000157.

[37] S. Santos, V. Barcons, H.K. Christenson, J. Font, N.H. Thomson, The intrinsic resolution limit in the atomic force microscope: implications for heights of nano-scale features, PLoS One 6 (2011) e23821, , https://doi.org/10.1371/journal.pone.0023821.